Structure *14*, 367–378, February 2006 ©2006 Elsevier Ltd All rights reserved DOI 10.1016/j.str.2005.11.008

Crystal Structure of the Human Retinitis Pigmentosa 2 Protein and Its Interaction with Arl3

Karin Kühnel,[1,3] Stefan Veltel,[1] Ilme Schlichting,[2] and Alfred Wittinghofer[1,*]

[1]Max-Planck-Institut für Molekulare Physiologie
Abteilung Strukturelle Biologie
Otto-Hahn-Strasse 11
44227 Dortmund
Germany

[2]Max-Planck-Institut für Medizinische Forschung
Abteilung Biomolekulare Mechanismen
Jahnstrasse 29
69120 Heidelberg
Germany

Summary

The crystal structure of human retinitis pigmentosa 2 protein (RP2) was solved to 2.1 Å resolution. It consists of an N-terminal β helix and a C-terminal ferredoxin-like α/β domain. RP2 is functionally and structurally related to the tubulin-specific chaperone cofactor C. Seven of nine known RP2 missense mutations identified in patients are located in the β helix domain, and most of them cluster to the hydrophobic core and are likely to destabilize the protein. Two residues, Glu138 and the catalytically important Arg118, are solvent-exposed and form a salt bridge, indicating that Glu138 might be critical for positioning Arg118 for catalysis. RP2 is a specific effector protein of Arl3. The N-terminal 34 residues and β helix domain of RP2 are required for this interaction. The abilitities of RP2 to bind Arl3 and cause retinitis pigmentosa seem to be correlated, since both the R118H and E138G mutants show a drastically reduced affinity to Arl3.

Introduction

Retinitis pigmentosa (RP) comprises a large group of heterogeneous diseases that results in progressive retinal degeneration and is the leading cause of hereditary blindness in humans. The prevalence of RP within the population is 1:3000–1:5000 (Haim, 2002). Mutations in more than 30 genes are known to cause RP (RetNet: http://www.sph.uth.tmc.edu/Retnet/home.htm). Most of the proteins encoded by these genes are involved in photoreception and transduction, but genes encoding transcription factors, and proteins involved in protein folding and trafficking, are also affected (Farrar et al., 2002). RP with an X-linked hereditary pattern causes the most severe forms of the disease. Approximately 10%–15% of the X-linked RP cases are caused by mutations in the retinitis pigmentosa 2 protein (RP2) (Schwahn et al., 1998; Hardcastle et al., 1999). RP2 encodes a protein of 350 residues and is ubiquitously expressed in all tissues at a low level (Schwahn et al., 1998; Chapple et al., 2000). It is both myristoylated and palmitoylated at the N terminus and is located at the plasma membrane. A deletion of Ser6 in RP2, which is known to cause RP, interferes with the targeting of the protein to the plasma membrane (Chapple et al., 2000).

The function of RP2 is still not well understood. It is a functional and structural homolog of the tubulin-specific chaperone cofactor C, and it has a sequence identity of 30.4% over a range of 151 amino acids (RP2 residues 42–192) (Schwahn et al., 1998). Cofactors A–E participate in tubulin folding. After the release of newly synthesized α- and β-tubulin subunits from the the cytosolic chaperonin TRIC/CCT, α- and β-tubulin folding intermediates form a complex with cofactors C, D, and E. Cofactors C and D together stimulate GTP hydrolysis by β-tubulin. The GTPase activating protein (GAP) activity of cofactors C and D is further enhanced by cofactor E. GTP hydrolysis triggers the release of the native tubulin heterodimer from the supercomplex (Tian et al., 1995, 1996, 1997, 1999). Together with cofactor D, RP2 also stimulates the GTPase activity of β-tubulin, but, unlike cofactor C, RP2 cannot substitute for cofactor C in the tubulin heterodimer assembly pathway (Bartolini et al., 2002). A conserved arginine in cofactor C has been postulated to act as an arginine-finger in the GTP hydrolysis of tubulin, analogous to the arginine-finger in RasGAP (Scheffzek et al., 1997). The R262A mutation in cofactor C abolishes its GAP activity. This arginine is conserved in RP2 (Arg118), and the mutation of Arg118 to His found in RP patients (Schwahn et al., 1998; Sharon et al., 2000) results in a protein with no GAP activity (Bartolini et al., 2002).

The GTP binding proteins Arl2 and Arl3 (Arf-like) are closely related members of the Arf (ADP ribosylation factor) subfamily of the Ras-related protein superfamily. Arl2 was identified in *S. cerevisae* as a chromosome instability mutant, Cin4 (Hoyt et al., 1990). A homolog of Arl2 in *C. elegans*, evl-20, associates with microtubules and was proposed to regulate cytoskeletal dynamics during cytokinesis and morphogenesis (Antoshechkin and Han, 2002); mutations of this gene in *Arabidopsis thaliana* disrupt microtubules (Mayer et al., 1999). Arl2 interacts with cofactor D (Shern et al., 2003; Bhamidipati et al., 2000), and it was shown that Arl2 downregulates the tubulin GAP activities of cofactors C, D, and E (Bhamidipati et al., 2000), but does not bind RP2 (Bartolini et al., 2002). Arl3, on the other hand, binds to RP2 in an apparent GTP-dependent manner, and it does not interact with cofactor C (Bartolini et al., 2002). Myristoylation of RP2 weakens the binding of Arl3 to RP2, leading to the proposal that Arl3 might bind unmodified RP2 in vivo and facilitate its targeting for modification (Bartolini et al., 2002).

Arl3 is localized to microtubule structures throughout the retina and is present at high concentration in the connecting cilium of photoreceptors. The connecting cilium is a thin bridge connecting the cell body and the outer segment of photoreceptors and plays an important role in the trafficking of proteins from the inner to

*Correspondence: alfred.wittinghofer@mpi-dortmund.mpg.de
[3]Present address: Max-Planck-Institut für Medizinische Forschung, Abteilung Biomolekulare Mechanismen, Jahnstrasse 29, 69120 Heidelberg, Germany.

the outer segments of photoreceptors. In contrast, RP2 is located at the plasma membrane throughout the photoreceptor cells and is not enriched in any photoreceptor organelle (Grayson et al., 2002). In analogy to the role of Arf proteins in cellular transport reactions, Arl3 and RP2 might be involved in protein trafficking in general or photoreceptor maintenance in particular.

Additional connections between retinal degeneration and Arl proteins have been documented. Mutations in Arl6 cause the Bardet-Biedl syndrome, which is characterized by severe symptoms including blindness and obesity. The *C. elegans* Arl6 homolog is expressed in ciliated cells and undergoes intraflagellar transport (Fan et al., 2004). Both Arl2 and Arl3 interact with the δ subunit of rod-specific cyclic GMP phosphodiesterase (PDEδ), which has been implicated in transport and membrane targeting of prenylated proteins toward the outer segments of rod and cones (Linari et al., 1999a). PDEδ was also shown to bind to retinitis pigmentosa GTPase regulator (RPGR), whose gene, RP3 (Meindl et al., 1996; Roepman et al., 1996), causes another X-linked form of the disease (Linari et al., 1999b). RPGR is targeted to the connecting cilium by the RPGR-interacting protein (RPGRIP) (Zhao et al., 2003).

Here, we report the crystal structure of human RP2. The interactions between RP2 and Arl3 were quantitatively characterized with purified proteins. RP2 is a bona fide effector of Arl3. The N-terminal 34 residues and β helix domain of RP2 are required for binding of Arl3. The RP2 patient mutations R118H and E138G show a drastically reduced affinity toward Arl3, indicating that failure of RP2 to bind Arl3 seems to cause retinitis pigmentosa.

Results

The N-Terminal β Helix Domain

The crystal structure of human retinitis pigmentosa 2 protein (RP2) was solved to 2.1 Å. The phasing was done with the multiwavelength anomalous diffraction (MAD) technique with selenomethionine-substituted protein crystals (Table 1). The model comprises 312 residues, but the N-terminal 33 residues are not visible in the electron density. The protein consists of an N-terminal β helix domain (1–228) and a C-terminal ferredoxin-like α/β domain (229–350) (Figure 1A). The parallel β helix domain is right-handed and consists of seven coils. It has the overall shape of a rectangular barrel with a diameter of approximately 10 Å × 20 Å and a height of roughly 30 Å. The first six coils are regular and consist of three short strands, a, b, and c, each of which forms a parallel β sheet with the corresponding strands from the other coils (Figures 1A and 1C). According to the nomenclature first introduced for pectate lyase (Yoder et al., 1993) and its adaptation for the C-terminal domain of the cyclase-associated protein (C-CAP) structure (Dodatko et al., 2004), these sheets are denoted as PB1, PB1a, and PB2. Strands a and c are 4–6 residues long, and strand b consists of two amino acids. The first 6 coils contain 19 residues on average, and 2 adjacent coils are separated by 4.7 Å, corresponding to an average β helix rise of 0.25 Å per residue. The first six coils of the β helix superimpose onto each other with an rmsd of 1.0 Å when the variable regions are omitted.

Table 1. Crystallographic Data Collection and Refinement Statistics

Data Collection		
Space group	$P3_221$	
Cell dimensions		
a, b, c (Å)	81.3, 81.3, 106.1	
α, β, γ (°)	90, 90, 120	
	Peak	Inflection
Wavelength (Å)	0.97923	0.97980
Resolution (Å)	20.0–2.10 (2.16–2.10)	20.0–2.10 (2.16–2.10)
R_{sym} (%)	4.5 (21.6)	5.0 (27.4)
$I/\sigma(I)$	21.1 (6.9)	18.7 (5.9)
Completeness (%)	97.9 (88.7)	98.6 (97.4)
Redundancy	5.7 (5.6)	5.8 (5.7)
Phasing		
Se sites	4	
FOM (acentric/centric)	0.510/0.271	
Refinement		
Number of reflections	24,149	
R_{work}/R_{free} (%)	19.7/23.5	
Number of atoms		
Protein	2,399	
Water	144	
B factors (Å^2)		
Protein	32.2	
Water	36.1	
Rms deviations		
Bond lengths (Å)	0.016	
Bond angles (°)	1.49	

Data in parentheses correspond to the highest-resolution bin.

The RP2 β helix domain is similar to that of *S. cerevisiae* C-CAP (Dodatko et al., 2004). Despite the low sequence identity of 11% between the C-CAP (368–508) and RP2 β helix domains (34–191), the structures superimpose with an rmsd of 2.1 Å (Figure 1B). Both proteins differ in their oligomerization states. C-CAP forms a strand-exchanged dimer, whereas RP2 is monomeric.

Quite unlike other β helix proteins, coils 6 and 7 of RP2 are connected by a very long loop (146–173) that covers almost one complete face of the β helix domain. This loop region contains a short helix, α_n0 (154–161), which contacts β helix coils 2 and 3. The β helix coil 7 is irregular and does not contain strand b, and the residues connecting a and c are disordered. Sequence comparison (Figure 2A) shows that, relative to RP2, cofactor C has a 3 residue insertion in this loop. But, since strands a and c participate in sheets PB1 and PB2, coil 7 is considered to be part of the β helix domain.

The extensive main chain hydrogen bond network within the three β sheets causes the stacked arrangement of the side chains (Figure 1D), both on the surface and within the core of the β helix. The core of this domain is tightly packed and mainly hydrophobic. There is no hydrophobic pocket that could fit a farnesyl or geranyl moiety as in the Arl2/3 effector PDEδ (Hanzal-Bayer et al., 2002). Only one water molecule is buried in the core of the β helix domain. This water is located between coils 2 and 3. It is stabilized by hydrogen bonds, which are formed with the carbonyl oxygen of Asp76 and the hydroxyl side chain of Ser78.

At right angles to the long axis of the β helix, the PB1 and PB2 side chains of each coil point toward each other and are involved in forming the hydrophobic core, as

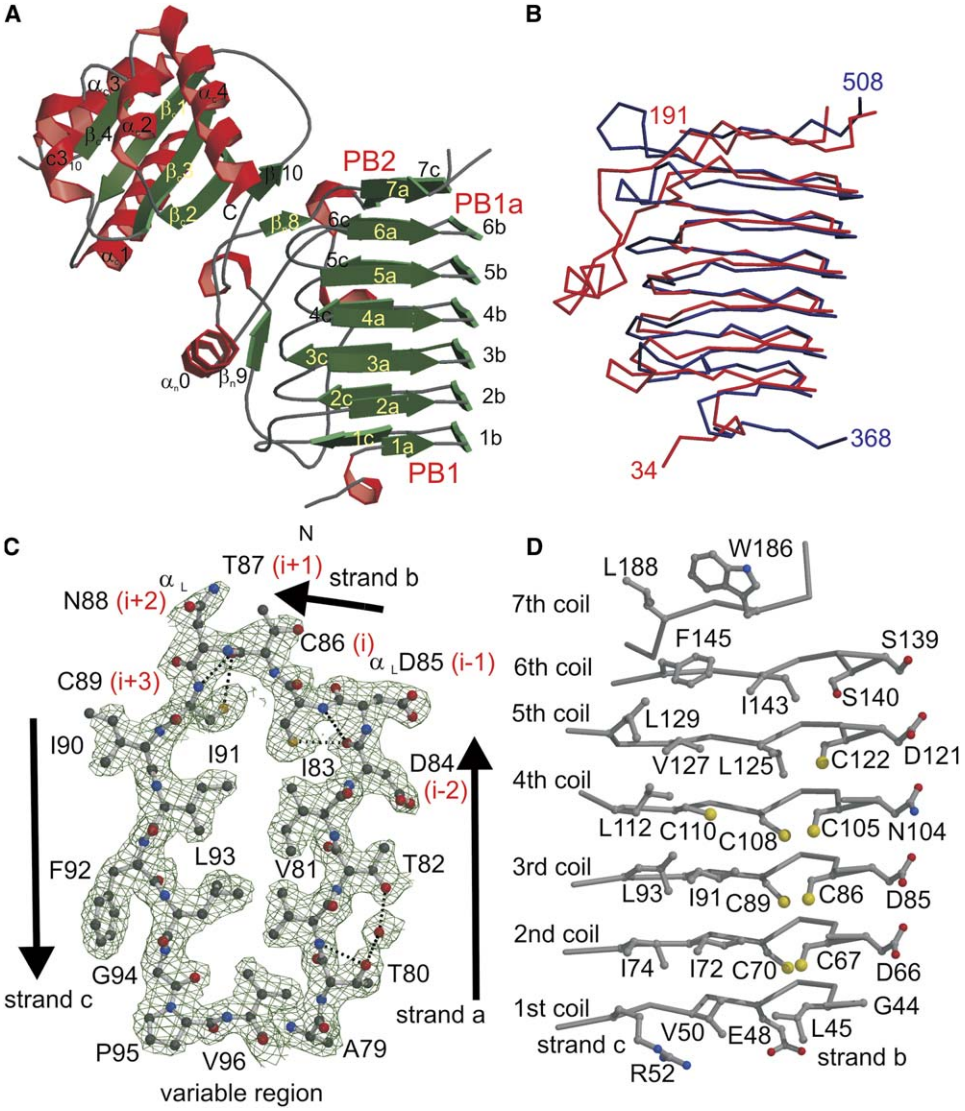

Figure 1. Structure of RP2

(A) Ribbon diagram of RP2, with green β strands, red α helices, and gray loop regions. In the N-terminal β helix domain, strands a, b, and c form the parallel β sheets PB1, PB1a, and PB2. The C-terminal α/β domain has a ferredoxin-like fold. The model includes residues 34–347.

(B) Cα chain traces of the superimposed β helix domains from RP2 (red) and C-CAP (blue).

(C) Details of the β helix fold. A horizontal cross-section of RP2 around coil 3 shows a rectangular shape of the β helix; hydrophobic and hydrophilic interactions stabilize the fold. Asp85 and Asn88 both adopt a left-handed α-helical conformation. The final $2F_o - F_c$ electron density is shown (contour level $\sigma = 1.0$).

(D) Vertical (along the helical axis) cross-section of the β helix domain, showing strands b and c and the corresponding sheets PB1a and PB2, respectively. Side chains inside the core and residues pointing toward the solvent are stacked in a ladder-like fashion.

shown for coil 3 (Figure 1C). Along the axis of the β helix, there are stacks of hydrophobic, mostly aliphatic side chains, which include residues Phe42-Ile64-Ile83-Phe102-Val119-Ile137 in PB1 and Val50-Ile72-Ile91-Cys110-Val127-Phe145 in PB2 (Figure 1D), where Phe42 points toward Val50 and Ile64 faces Ile72, etc. The two other ladders include residues Phe62-Val81-Val100-Phe117-Pro135 in PB1 and Ile74-Leu93-Leu112-Leu129 in PB2. In addition, there are two ladders within the core of the β helix consisting of weakly hydrophobic/hydrophilic side chains, with a high incidence of cysteines: Leu45-Cys67-Cys86-Cys105-Cys122-Ser140 are the first residues of strand b. Glu48-Cys70-Cys89-Cys108-Leu125-Ile143 form the second hydrophilic ladder and correspond to the first residues of strand c. The interactions of the side chains of these hydrophilic residues appear to be important for the stabilization of the β helix.

Strands a/b and b/c of the β helix domain are separated by 1 residue, and only 3 residues are required to make turns of roughly 90° (Figure 1C). The amino acids connecting these strands adopt a left-handed α-helical conformation, and their side chains point toward the solvent. The tight turn between strands a and b is stabilized by a weak hydrogen bond formed between the thiol group of the first residue of strand b, denoted as i, (or the hydroxyl side chain in the case of Ser140 in coil 6) and the main chain carbonyl oxygen of residue i−2.

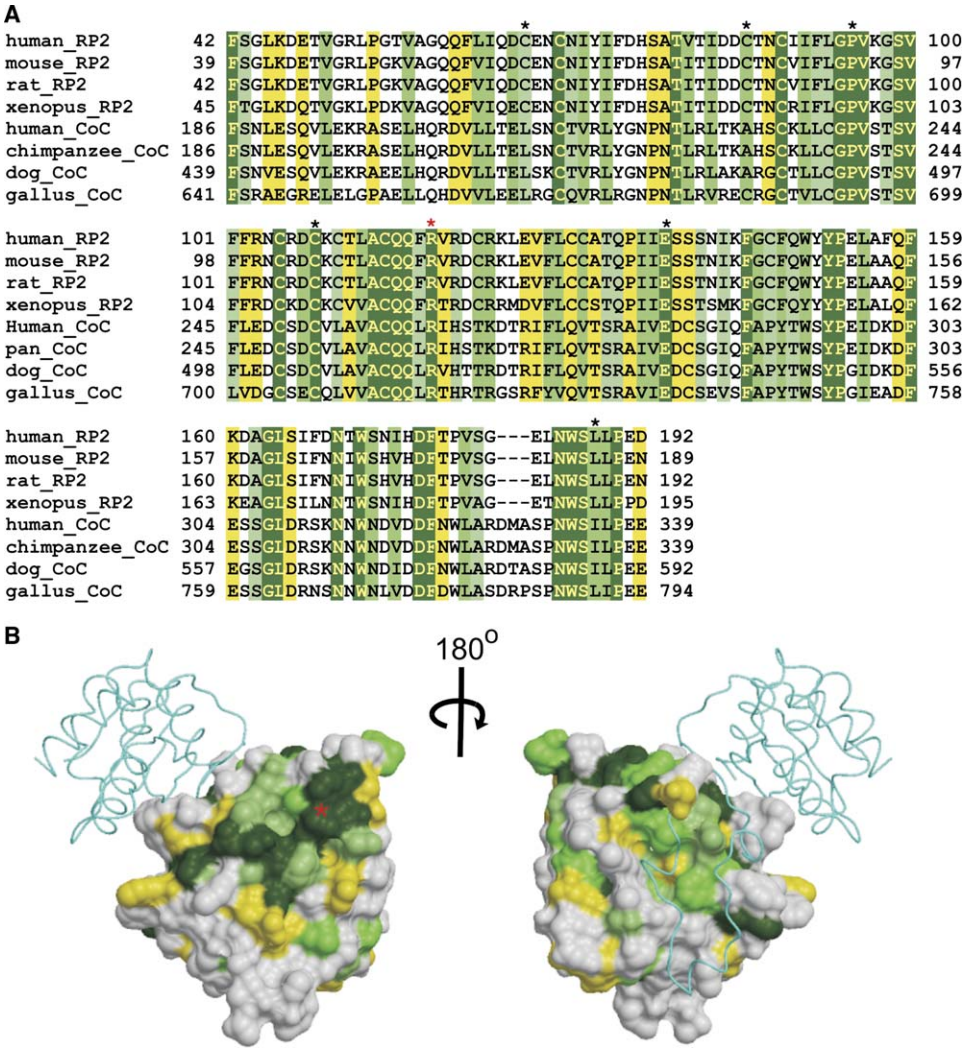

Figure 2. Sequence Conservation between the N-Terminal β Helix Domain of RP2 and the C-Terminal Domain of Cofactor C

(A) Alignment of amino acid sequences of human RP2 (O75695, Swiss-Prot), mouse RP2 (Q9EPK2, TrEMBL), rat RP2 (XM_346266, NCBI), *Xenopus* RP2 (BC04122, NCBI), and cofactor C of human (Q15814, Swiss-Prot), chimpanzee (XM_518477, NCBI), dog (XM_538923, NCBI), and chicken (XM_426123, NCBI) are shown. Conserved residues are highlighted, with the degree of conservation decreasing from dark green to yellow. Sequence alignment was done with ClustalW (Higgins et al., 1996), and analysis of the degree of conservation was done with AMAS (Livingstone and Barton, 1993). Missense mutations identified in retinitis pigmentosa patients are marked with an asterisk. The catalytically important residue Arg118 is labeled in red.

(B) Surface representation of the β helix domain with surface residues of the β helix domain color coded according to their degree of conservation as in (A); the front side is on the left, and the less-conserved back side is on the right. The position of Arg118 is marked with a red asterisk. The backbone of the C-terminal domain is shown in blue.

The formation of hydrogen bonds between the side chain of residue i and the carbonyl oxygens of i−2 has been previously observed in the C-CAP structure (Dodatko et al., 2004). The exception is the a/b turn in RP2 coil 1, where Leu45 occupies position i and shields the core of the β helix domain from the solvent. Leu45 is incapable of forming a stabilizing hydrogen bond. Gly44 is located at position i−1, and, as a consequence, this turn might be less strained compared to other turns, where a nonglycine amino acid has to adopt the left-handed α-helical conformation; thus, additional stabilization through a hydrogen bond is not necessarily required. In contrast to the C-CAP structure, additional hydrogen bonds are observed in three of the b/c turns of RP2. The thiol group of residue i+3, the first residue of strand c, forms a weak hydrogen bond with the main chain carbonyl oxygen of the second residue in strand b (i+1). The cysteine residues at positions i and i+3 would, in principle, be capable of forming disulfide bridges with each other, but no disulfide bridges are visible in the electron density.

The β helix domains of RP2 and cofactor C share a sequence identity of 30%. The conservation of the surfaces of the two proteins is highest in the region surrounding Arg118 and on the more C-terminal part of the β helix domain, arguing that this is the site of functional interactions (Figure 2B). Both proteins show less similarity in the N-terminal part and the side of the domain opposite of Arg118. This degree of conservation in the region of the catalytically important Arg118 further

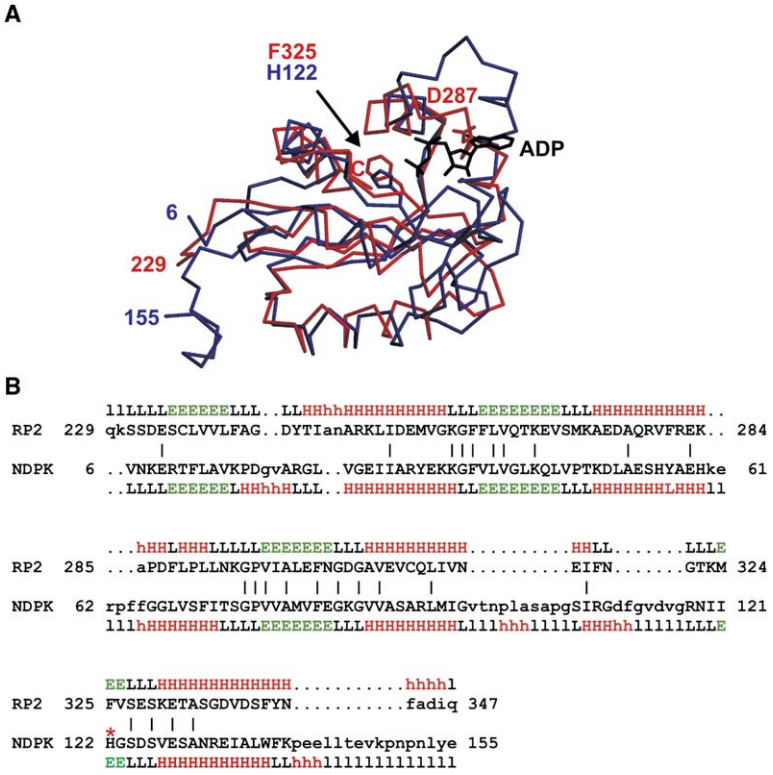

Figure 3. Comparison between the C-Terminal RP2 Domain and NDP Kinase

(A) Superimposition of Cα chain traces of the C-terminal RP2 domain (red, residues 229–347) and *Dictyostelium* NDP kinase (blue, residues 6–155, PDB code: 1hiy) with bound 3′deoxy-3′amino-ADP (black) is shown. The transiently phosphorylated His122 in NDP kinase is replaced by Phe325 in RP2; the side chain of Asp287 of RP2 would clash with the sugar moiety of ADP.

(B) Structure-based sequence alignment between the C-terminal RP2 domain and NDP kinase. The catalytically important residue His122 of NDP kinase is labeled with a red asterisk. Secondary structure elements of both structures are shown, and identical residues are marked. Superimposition and sequence alignment were done with DaliLite (Holm and Park, 2000).

supports the idea of one common functional role of RP2 and cofactor C.

The C-Terminal Ferredoxin-like α/β Domain

The C-terminal α/β domain (229–350) has a ferredoxin-like fold (Figure 3). It forms a three-layered α+β sandwich with an antiparallel β sheet with the strand order of β_c2-β_c3-β_c1-β_c4 in the sheet, and it is surrounded by 4 α helices and a short 3_{10} helix on both sides. A DALI search (Holm and Sander, 1993) showed that the C-terminal domain is structurally very similar to nucleoside diphosphate (NDP) kinase (Figure 3A). The C-terminal β strands and α helices 1, 3, and 4 of RP2 superimpose with an rmsd of 2.2 Å onto the *Dictyostelium* NDP kinase (PDB code: 1npk). A structure-based sequence alignment of RP2 and NDP kinase is shown in Figure 3B. The sequence identity between both domains is 22%. NDP kinase catalyzes the phosphorylation of nucleoside diphosphates to triphosphates. The reaction involves a two-step phosphotransfer reaction with a covalent intermediate in which the active site residue His122 is phosphorylated. Despite the general structural similarity of NDP kinase and the RP2 C-terminal domain, there are significant differences around the NDP kinase active site, since residues required for NDP kinase activity are not conserved in RP2. The transiently phosphorylated residue His122 is replaced by Phe325 in RP2. No other histidines are present in the neighborhood of Phe325. Asp287 of RP2 would clash with the sugar moiety of the bound nucleotide from NDP kinase. No bound ligands are visible in the RP2 electron density. Furthermore, no binding of ADP to RP2 could be detected by isothermal calorimetry (data not shown). This result and the large differences between the active site of NDP kinase and the corresponding residues in the C-terminal domain of RP2 indicate that RP2 should have no NDP kinase-like phosphotransferase activity. The function of the C-terminal domain thus remains undefined.

The Catalytically Active Arg118

Arg118 in coil 5 in the β helix domain is solvent accessible (Figures 4A and 4B). It is conserved throughout different species in both RP2 and cofactor C, and the neighboring hydrophobic residues Phe177, Ile136, and Phe101 are also conserved (Figure 2A). Next to Arg118 in coil 5 are the conserved Gln116 and Arg120. Arg120 is conserved in RP2, but it is replaced by a histidine in cofactor C. The unconserved Arg103 is the second arginine in the proximity of Arg118. Two conformations of Arg118 are visible in the electron density. The guanidinium group of Arg118 of the major conformer (60% occupancy) forms a hydrogen bond with two waters, one of which forms hydrogen bonds with the side chain of Thr133, and the carbonyl oxygen of Gln134. An acidic residue close enough to Arg118 to form a salt bridge is Glu138. In the major conformer, the side chain of Arg118 points away from Glu138, while the second conformer forms a salt bridge with Glu138 (distance 3.4 Å). The proposal that Glu138 has an important functional role, such as to position Arg118 for catalysis, is strengthened by the observation that Glu138 is mutated in retinitis pigmentosa (see below). In the crystal, the salt bridge forming conformation is less occupied (40% occupancy), most likely due to the close proximity of Leu313 of a symmetry-related molecule; there is a distance of 3.4 Å between the methyl group of Leu313 and the guanidinium group of Arg118.

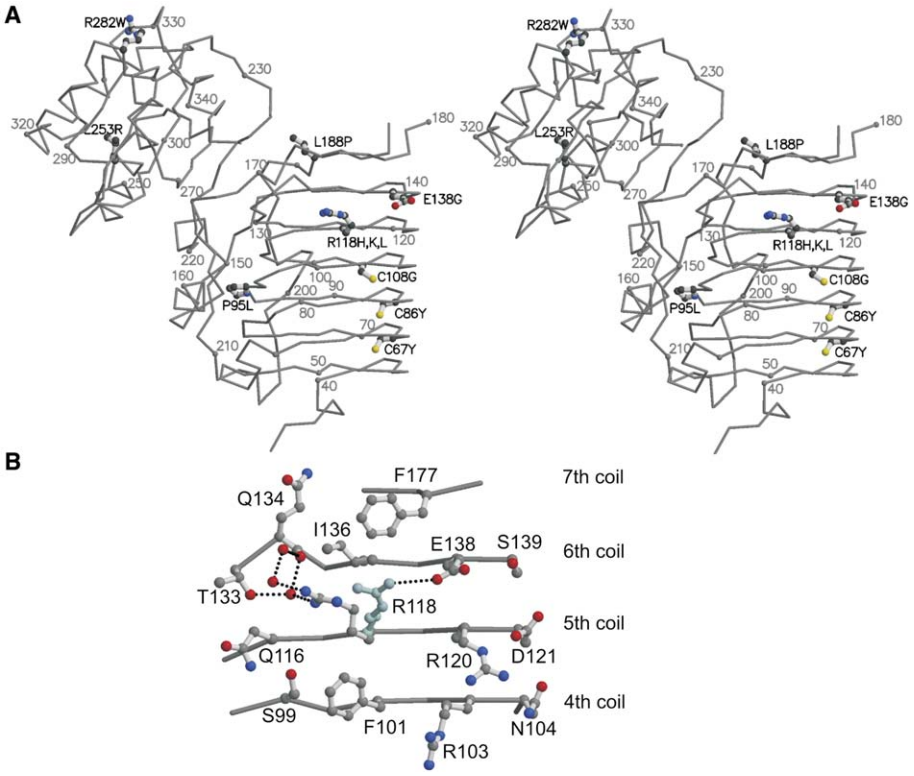

Figure 4. Patient Mutations in RP2

(A) Stereoview of the Cα backbone of RP2; every tenth Cα atom is labeled. Side chains of residues mutated in RP patients and corresponding missense mutations are included.

(B) Localization and interaction of Arg118, a residue essential for the GAP activity of the tubulin cofactor C, and RP2, which is frequently mutated in RP. Hydrogen bonds between the arginine side chain and nearby waters are shown. The second lower occupied conformation of Arg118 is shown in light blue and forms a salt bridge with Glu138, which is also mutated in RP.

RP2 Mutations

Many of the mutations identified in retinitis pigmentosa patients are insertions and deletions, which result in frameshifts and/or premature truncation of the protein, with a loss of function of RP2 in the affected individuals (Breuer et al., 2002; Mears et al., 1999; Miano et al., 2001). The most prevalent mutation is a point mutation yielding a premature termination at Arg120 (Mears et al., 1999; Vorster et al., 2004). A deletion of three bases, 409–411, retains the reading frame but causes a deletion of Ile137 (Sharon et al., 2000). This residue is located in strand 6a, and its deletion likely destabilizes the β helix domain.

Missense mutations are known for nine amino acids and are shown in Figure 4A. Some of them cluster to the hydrophobic core and would be expected to destabilize the protein. Seven of the affected amino acids are located in the β helix domain. Mutations of Cys67 and Cys86, the first residues of strand b in coils 2 and 3, respectively, to the aromatic tyrosine (Breuer et al., 2002; Sharon et al., 2000) disturbs the tight hydrophobic core packing around these cysteines, and it may additionally destabilize the core due to the loss of a (albeit weak) hydrogen bond between the thiol side chain and the carbonyl oxygen of residue i−2. Creation of a cavity by the C108G mutation (Mears et al., 1999) inside the tightly packed hydrophobic core of the β helix domain is presumably also destabilizing. This mutant is further destabilized because, unlike the thiol side chain, glycine cannot form a hydrogen bond with the carbonyl oxygen of the second residue of strand b. Pro95 is highly conserved in RP2 and cofactor C. It is situated in a tight turn, which is stabilized by a hydrogen bond between the carbonyl oxygen of Gly94 and the amide nitrogen of Val96. The P95L mutation (Sharon et al., 2000) would cause clashes with Phe159 in helix α_n0 and the side chain of Leu164 (both residues are conserved in RP2 of different species).

The side chain of Leu188, conserved in RP2, is in van der Waals contact with Trp171 and Trp186 and favorably interacts with the hydrophobic part of the Arg228 side chain. The L188P mutation (Breuer et al., 2002) probably destabilizes the loop (188–192), which connects the last strand of the β helix domain with the C-terminal domain. Leu253 is located in helix α_c1 of the C-terminal domain. It is part of the hydrophobic core and interacts with hydrophobic side chains from helix α_c3 and strands β_c1 and β_c3. The mutation of Leu253 to arginine (Wada et al., 2000) would cause severe clashes in hydrophobic core packing.

Of particular interest are mutations of surface-exposed residues, because they might be involved in interactions of RP2 with its binding partners (see below). The R282W mutant, although identified in RP patients (Miano et al., 2001), has been suggested to be a low-frequency polymorphism (1.7%) rather than a disease

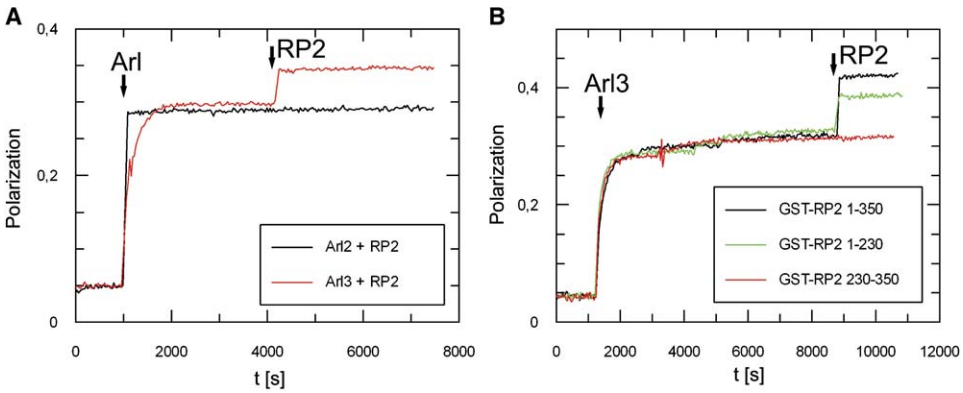

Figure 5. Arl3 Binds to the N-Terminal Domain of RP2

(A) RP2 is specific for Arl3. A total of 200 μM nucleotide-free Arl2 (black) or Arl3 (red) was added to 1 μM mGppNHp to saturate the nucleotide with protein. After equilibration, 10 μM RP2 was added, which yields an additional increase in polarization for Arl3, but not for Arl2.

(B) Binding of Arl3 to the N terminus of RP2. A total of 200 μM nucleotide-free Arl3-His protein was added to 1 μM mGppNHp in several steps to reach saturation. As indicated, 10 μM full-length RP2, N-terminal domain, or C-terminal domain as GST fusion constructs were added. An increase of polarization could only be observed for the full-length protein or the N-terminal domain.

variant (Thiselton et al., 2000). It is striking that Arg282 is the only nonglycine outlier in the Ramachandran plot. The electron density of this residue is well defined. Arg282 is located in a tight turn connecting helices $\alpha c3_{10}$ and $\alpha_c 2$ and is stabilized by a complex network of hydrogen bonds. Since Arg282 is not well conserved and is replaced by glutamine in mouse, gallus, and *Xenopus*, it is apparently not crucial for interactions with other proteins.

The presumed catalytically important and invariant residue Arg118 is mutated to Leu, His, Lys, or Cys in many RP patients (Breuer et al., 2002; Miano et al., 2001; Schwahn et al., 1998; Bader et al., 2003). Glu138, which is also conserved between RP2 and cofactor C, is located in the vicinity of Arg118 and is capable of forming a salt bridge with Arg118. The E138G mutation (Miano et al., 2001) should have no detrimental effect on the overall stability of RP2, but Glu138 might be critical for positioning Arg118 for catalysis, or it may affect some other properties of the protein.

Quantitative Evaluation of RP2-Arl3 Binding

In order to relate the structural findings with the biochemistry, we needed to set up a quantitative assay for the interaction between RP2 and Arl proteins. Binding of RP2 to Arl was followed by a fluorescence polarization assay. Binding of the fluorescent GTP analog mGppNHp to the small GTP binding protein Arl3 (21 kDa) leads to an increase of polarization. Further addition of RP2 (40 kDa) or GST-RP2 (66 kDa) to Arl3-mGppNHp results in an additional increase of polarization due to the formation of a higher molecular mass complex. As a control, we repeated the experiments with Arl2, which showed an increase in polarization upon binding to mGppNHp, but no further increase upon addition of RP2. We could thus confirm previous results from pull-down experiments that showed that RP2 binds specifically to Arl3 and not to Arl2 (Bartolini et al., 2002) (Figure 5A). Although we cannot exclude weak binding of RP2 to excess Arl3, this binding is specific for the nature of the nucleotide, as no increase in polarization to Arl3-mGDP could be observed (also see below).

To determine the equilibrium binding affinity between Arl3 and RP2, and to show that RP2 is a bona fide effector of Arl3, an equilibrium titration was performed by using a constant concentration of Arl3 bound to mant-nucleotides (excess Arl3, 1 μM nucleotide) and increasing concentrations of RP2 protein. The increase of polarization was fitted by a binding equation. The K_d value for Arl3-mGppNHp and RP2 is 64 nM (Figure 6A). The affinity of RP2 to the GDP bound form of Arl3 is about 400-fold weaker (Figure 6B), similar to what has been found for other G protein-effector interactions in which differences in affinity in the order of 1000-fold were measured (Rudolph et al., 2001; Rose et al., 2005).

Previously, it has been observed that binding of effectors to GTP binding proteins stabilizes guanine nucleotide binding, and that such GDI (guanine-nucleotide dissociation inhibitor) effects can be used to quantitatively measure binding affinities (Rudolph et al., 2001). For RP2, we could also show that it acts as a GDI for the GTP bound form of Arl3. With increasing amounts of RP2 in the assay, we observed decreasing dissociation rate constants of mGppNHp from Arl3 (Figure 6C). The dissociation rates, k_{obs}, were plotted against the RP2 concentrations. We determined the affinity between Arl3-mGppNHp and RP2 to 92 nM, which is in the same range as the value obtained from polarization experiments. The dissociation rate constant of mGppNHp from Arl3 is 3.5×10^{-4} s^{-1} and is reduced 10-fold (4.4×10^{-5} s^{-1}) when Arl3-mGppNHp is saturated with RP2. Since only mGppNHp bound Arl3 was monitored in the GDI assay, and the binding affinity is in the same range as that obtained by the direct equilibrium binding method, we can exclude that nucleotide-free Arl3 has a measurable binding affinity for RP2 in our assay conditions.

The N-Terminal Domain Is Sufficient for Arl Binding

It was investigated whether both domains of RP2 are required for binding of Arl3-GTP. The N- and C-terminal domains (amino acids 1–230, amino acids 230–350) were expressed and used as GST fusion proteins, since they were less stable than the full-length protein. An

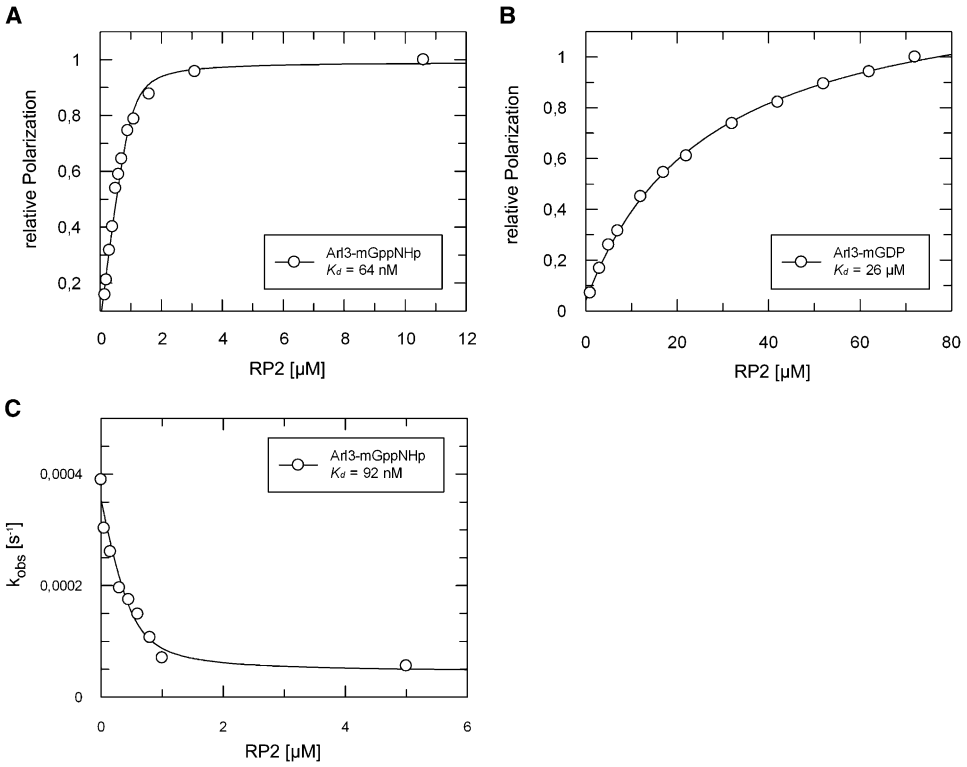

Figure 6. Equilibrium Binding Measurements of the RP2-Arl3 Interaction

(A and B) A total of 1 μM (A) Arl3-mGppNHp or (B) Arl3-mGDP was titrated with increasing amounts of RP2, and the increase in polarization was plotted against the RP2 concentration. Data were fitted to a quadratic equation to determine the equilibrium dissociation constants.

(C) Inhibition of the nucleotide dissociation from Arl3 protein by the interaction with RP2. The observed dissociation rates of mGppNHp from Arl3 were plotted against the RP2 concentrations used in the GDI assay. The concentration of Arl3-mGppNHp was 500 nM. The curve was fitted with a single exponential equation to determine the equilibrium dissociation constant.

increase of polarization could be detected only after addition of the N-terminal domain, but not of the C-terminal domain (Figure 5B). The smaller increase of polarization due to the N-terminal domain compared to the full-length construct is due to the lower molecular mass of the former. We conclude that Arl3 binds to the part of RP2 homologous to cofactor C, and that the C-terminal part is not required for binding.

Since the first 33 N-terminal amino acids of RP2 are not visible in the structure, the importance of these residues for Arl3 binding was analyzed. A deletion mutant lacking the first 34 amino acids (RP2 Δ34) was tested in the polarization assay and showed an affinity to Arl3-mGppNHp of 19 μM, roughly 300-times lower than full-length RP2 (Figure 7A). The CD spectra of full-length and truncated RP2 show no significant differences (Figure 7B).

Effect of Patient Mutations on RP2-Arl3 Binding

As deduced from the structure and discussed above, most of the mutations in RP2 are likely to destabilize the protein, rather than to influence the biochemistry of RP2. In contrast, mutations on the surface might influence interactions with binding partners. R118H was one of the first RP2 mutations discovered in patients (Schwahn et al., 1998). We tested the affinity of this and two other surface mutations, E138G and R282W, for their interactions with Arl3. Substantiating earlier qualitative observations (Bartolini et al., 2002), we found that R118H reduces the affinity of RP2 for Arl3 by over 800-fold (Figure 7A), with a K_d of 52 μM, which is even lower than what is found for the interaction of wild-type RP2 with Arl3-GDP. The E138G mutation decreases the affinity by 150-fold. This shows that the mutated proteins can no longer bind Arl3 with physiologically relevant affinities. The R282W mutation in the C-terminal domain of RP2 is not expected to affect the binding to Arl3 dramatically, since Arl3 does not require this domain for binding. In keeping with this prediction, the affinity of the R282W RP2 mutant for Arl3 is reduced only 3-fold compared to wild-type. To exclude that the dramatic effects on the binding interaction between Arl3 and RP2 are due to improper folding of the mutant protein, CD spectra of the wild-type and mutant proteins were recorded (Figure 7B). All of the mutant proteins show secondary structure elements similar to the wild-type protein; thus, one can conclude similar (i.e., proper) folding of the proteins.

Discussion

RP2 is a two-domain protein. The N-terminal β helix domain specifically interacts with Arl3, but not Arl2. RP2 is an effector of Arl3, since the interaction is specific for the GTP bound state of Arl3. In contrast, the homologous cofactor C does not bind Arl2, nor does it bind Arl3 (Bartolini et al., 2002). RP2 contains a C-terminal NDP kinase-like domain, but important catalytic residues

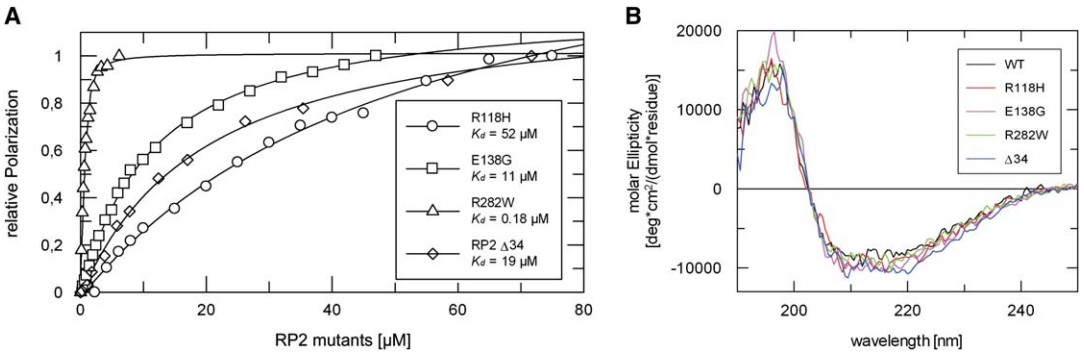

Figure 7. N-Terminal Deletion and RP Patient Mutations Affect the RP2-Arl3 Interaction

(A) Affinities of the RP2 mutants R118H, E138G, R282W, or RP2Δ34 to Arl3 were measured by fluorescence polarization as described for wild-type in Figure 6A. The measured K_d values for each mutant are shown.

(B) CD spectra of 2.5 μM wild-type and mutant RP2 in 5 mM K_2HPO_4/KH_2PO_4 (pH 7.4) at 20°C.

are not conserved in RP2; thus, the biological function of this domain remains unclear.

The N-terminal 34 residues of RP2 are also required for Arl3 binding, since their deletion severely weakens Arl3 binding. The N-terminal residues are not visible in the electron density because they were degraded during the 2 months it took the crystals to grow (data not shown). Secondary structure prediction with JPRED (Cuff et al., 1998) indicates that the 34 N-terminal residues are mainly disordered, and only residues 6–9 are expected to form a short α helix. Preliminary experiments suggest that binding of Arl3 might induce folding of the N-terminal stretch from RP2. Cofactor C and RP2 show a high degree of conservation in the region encoding the β helix domain, but cofactor C does not share homology with the N-terminal 34 residues. Instead, the β helix domain of cofactor C is located at the C terminus, and cofactor C contains an N-terminal spectrin-like coiled coil domain, which is expected to interact with other spectrin repeat-containing proteins (Grynberg et al., 2003). The specific binding of Arl3 for RP2 as compared to cofactor C thus appears to arise from the 34 N-terminal residues of RP2 that are absent in cofactor C.

Most of the missense mutations identified in retinitis pigmentosa patients are expected to have a destabilizing effect on the protein and might interfere with proper folding. The mutated residues Arg118 and Glu138 are located on the surface of the β helix domain. Based on the structure, we propose that Glu138 might have a role in positioning Arg118 for catalysis. Our affinity measurements also show that Glu138 and Arg118 are additionally involved in RP2 functioning as an effector protein for the GTP binding protein Arl3, implying that the abilities of RP2 to bind Arl3 and cause retinitis pigmentosa are correlated. How the function of RP2 in the folding of the α/β tubulin dimer and its ability to bind Arl3 are connected needs to be investigated further.

Experimental Procedures

Plasmid Constructs

Cloning of murine Arl2 and Arl3 has been described previously (Renault et al., 2001; Linari et al., 1999a). Arl2 and Arl3 were inserted as NcoI/XhoI fragments by PCR into the pET20 vector to produce His-tagged proteins. RP2 constructs (Schwahn et al., 1998) were cloned as BamHI/EcoRI (RP2 1–350, RP2 230–350 and RP2 Δ34) or BamHI/XhoI (RP2 1–230) fragments by PCR into pGEX-4T3 to express GST fusion proteins. The RP2 mutants R118H, E138G, and R282W were generated by using the QuikChange protocol (Stratagene). RP2 and Arl3 (Q71L) were coexpressed from a bicistronic pGEX-4T-1 plasmid (Amersham Biosciences), in which the N terminus of RP2 was fused to a GST tag between BamHI/EcoRI sites, and the GTPase-deficient Arl3 (Q71L) mutant was cloned behind RP2 without a tag at the EcoRI site. RP2 contains the D168N mutation, which is a polymorphism (Lin et al., 2001).

Protein Expression and Purification

Wild-type and mutant RP2 were expressed as GST fusion proteins from the pGEX-4T3 vector in the *E. coli* strain Rosetta BL21DE3. Cell lysate supernatant was applied to a GSH-column (Amersham Biosciences) preequilibrated with standard buffer (50 mM Tris [pH 7.5], 100 mM NaCl, 5 mM $MgCl_2$, 3 mM β-mercaptoethanol) at 4°C. Thrombin (Serva, Heidelberg) cleavage was performed on the column, and the eluted protein was purified by gel filtration on a Superdex S75 26/60 column (Amersham Biosciences) with standard buffer. Purified protein was concentrated, flash-frozen in liquid nitrogen, and stored at −80°C.

The truncated RP2 constructs GST-RP2 1–350, 1–230, and 230–350 were purified as described above by elution from the GSH-column with standard buffer plus 30 mM glutathione, without the proteolysis step. C-terminal His-tagged Arl2 and Arl3 were expressed in *E. coli* strain Rosetta BL21DE3. The supernatant of lysed cells was loaded onto a Ni-NTA column (QIAGEN). Proteins were eluted with standard buffer with 250 mM imidazol, followed by gel filtration on a Superdex 75 S26/60 column (standard buffer). To generate nucleotide-free Arl proteins, they were incubated with 1 U/mg alkaline phosphatase (Roche Diagnostics) in an exchange buffer (200 mM $[NH_4]_2SO_4$, 1 mM $ZnCl_2$) for 2 hr at 4°C. Dephosphorylation of nucleotides was monitored by HPLC. After dephosphorylation, Arl2/3 were separated from nucleosides and alkaline phosphatase through Ni-NTA chromatography.

Crystallography

The RP2-Arl3(Q71L) complex was coexpressed from a bicistronic plasmid. *E. coli* cells were grown in minimal medium containing selenomethionine as described (Van Duyne et al., 1993). The supernatant was loaded onto a GSH-Sepharose column, which was washed with 20 mM Tris (pH 7.5), 0.3 M NaCl, 5 mM $MgCl_2$, 10 mM DTE and thereafter treated with thrombin under continuous circulation overnight at 4°C. The liberated complex was eluted, concentrated, and applied onto a Superdex 200 HR16/60 column preequilibrated with 20 mM Tris (pH 7.5), 0.1 M NaCl, 5 mM $MgCl_2$, 10 mM DTE. The eluted complex was concentrated to 30 mg/ml, frozen, and stored at −80°C. HPLC analysis showed that the complex was loaded with GTP. Crystals were grown by the hanging drop method, and 3 μl 35 mg/ml protein solution was mixed with 3 μl of the reservoir solution (1.8 M $[NH_4]_2SO_4$, 0.1 M HEPES [pH 7.5]). Crystals grew after 2 months and were found to contain only RP2. Failure to obtain

crystals of the complex could have been due to (1) hydrolysis of GTP, (2) high salt concentration disrupting protein-protein interactions, or (3) degradation of the N terminus of RP2. HPLC analysis of the 2-month-old crystallization drops showed that the GTP was completely hydrolyzed, which caused a dissociation of the complex and thus enabled RP2 to crystallize alone. To investigate the protein content of the RP2 crystals, they were analyzed on an SDS gel, after washing with mother liquor and dissolving in water, and showed a shortened RP2 fragment (not shown) whose exact mass could not be determined by mass spectrometry. However, since the RP2 model is lacking only the three C-terminal residues, we conclude that the N terminus of RP2 was degraded. RP2 crystals were flash cooled in liquid nitrogen after transfer into 20% glycerol, 1.8 M $(NH_4)_2SO_4$, 0.1 M HEPES (pH 7.5). Diffraction data were collected on beamline X06SA at the SLS, Switzerland. Data were processed with XDS (Kabsch, 1993). The crystals belong to space group $P3_221$, with unit cell dimensions a = b = 81.5 Å, c = 105.9 Å and were diffracted to 2.1 Å. The structure was solved by two-wavelength MAD phasing with SHARP (de la Fortelle and Bricogne, 1997), automatic model building was done with ArpWarp (Perrakis et al., 1999), and refinement was carried out with Refmac5 (Murshudov et al., 1999). O was used for inspection of the electron density maps and manual rebuilding of the model (Jones et al., 1991). The N-terminal 33 residues, amino acids 181–183, and the C-terminal residues 348–350 are disordered.

Measurement of the Interaction between Arl3-mGppNHp and RP2

Polarization measurements were performed in a Fluoromax2 spectrometer (S.A. Instruments, USA), with excitation at 366 nm and emission at 450 nm. A total of 1 μM of the fluorescent GTP-analog mGppNHp (m, mant: N-methylanthraniloyl) was saturated with nucleotide-free Arl proteins until no further increase in polarization was obtained. For RP2 affinity measurements, increasing amounts of RP2 proteins were added. The increase in polarization upon addition of RP2 was integrated over at least 15 min, corresponding to at least 30 measured values. All measurements were performed in standard buffer including 0.005% Tween 20 at 10ºC. Data analysis, fitting, and plotting were done with the Grafit 5.0 program (Erithracus software, Horley, UK). K_d values were calculated as described elsewhere (Kraemer et al., 2001).

The affinity between Arl3-mGppNHp and RP2 was additionally determined by using the inhibition of the nucleotide dissociation from Arl3 by the binding of the effector RP2. The rate constants (k_{obs}) of the mGppNHp dissociation from Arl3 were measured in the presence of varying RP2 concentrations. mGppNHp (500 nM) was incubated in standard buffer with saturating amounts of nucleotide-free Arl3 and different RP2 concentrations, from 0 to 5 μM at 10ºC. The reaction was started by adding 1 mM GTP. The fluorescent decay was monitored in a Fluoromax2 spectrometer (S.A. Instruments, USA) with excitation and emission at 366 nm and 450 nm, respectively. The fluorescence spectra obtained were fitted by a single exponential function yielding the rate constant for the mGppNHp dissociation, k_{obs}. The calculated k_{obs} values were plotted against the concentration of RP2. K_d, k-RP2, and k+RP2 were calculated as described before (Herrmann et al., 1996).

Circular Dichroism

The secondary structures of wild-type and mutant proteins were investigated by circular dichroism. Spectra were recorded from 190 nm to 250 nm on a Jasco J-710 spectrometer (Japan Spectroscopic Co., Ltd., Tokyo, Japan). Samples were measured in cells of 0.1 cm path length at 20ºC. Data were collected with 0.5 nm bandwidth, 1 s time averaging, and a scanning speed of 50 nm/min. A total of 20 spectra were accumulated for each protein.

Acknowledgments

We thank D. Kühlmann and A. Scherer for technical assistance, Dr. I. Vetter for support of the crystallographic software, and Dr. B. Shoeman and Dr. A. Meinhart for advice. We are grateful to the staff of beamline X06SA at the Swiss Light Source for their support. We additionally thank Prof. Berger, Universität Zürich, for providing the RP2 clone. K.K. has been supported by the Peter and Traudl Engelhorn-Stiftung.

Received: August 31, 2005
Revised: October 24, 2005
Accepted: November 1, 2005
Published: February 10, 2006

References

Antoshechkin, I., and Han, M. (2002). The *C. elegans evl-20* gene is a homolog of the small GTPase ARL2 and regulates cytoskeleton dynamics during cytokinesis and morphogenesis. Dev. Cell *2*, 579–591.

Bader, I., Brandau, O., Achatz, H., Apfelstedt-Sylla, E., Hergersberg, M., Lorenz, B., Wissinger, B., Wittwer, B., Rudolph, G., Meindl, A., and Meitinger, T. (2003). X-linked retinitis pigmentosa: RPGR mutations in most families with definite X linkage and clustering of mutations in a short sequence stretch of exon ORF15. Invest. Ophthalmol. Vis. Sci. *44*, 1458–1463.

Bartolini, F., Bhamidipati, A., Thomas, S., Schwahn, U., Lewis, S.A., and Cowan, N.J. (2002). Functional overlap between retinitis pigmentosa 2 protein and the tubulin-specific chaperone cofactor C. J. Biol. Chem. *277*, 14629–14634.

Bhamidipati, A., Lewis, S.A., and Cowan, N.J. (2000). ADP ribosylation factor-like protein 2 (Arl2) regulates the interaction of tubulin-folding cofactor D with native tubulin. J. Cell Biol. *149*, 1087–1096.

Breuer, D.K., Yashar, B.M., Filippova, E., Hiriyanna, S., Lyons, R.H., Mears, A.J., Asaye, B., Acar, C., Vervoort, R., Wright, A.F., et al. (2002). A comprehensive mutation analysis of RP2 and RPGR in a North American cohort of families with X-linked retinitis pigmentosa. Am. J. Hum. Genet. *70*, 1545–1554.

Chapple, J.P., Hardcastle, A.J., Grayson, C., Spackman, L.A., Willison, K.R., and Cheetham, M.E. (2000). Mutations in the N-terminus of the X-linked retinitis pigmentosa protein RP2 interfere with the normal targeting of the protein to the plasma membrane. Hum. Mol. Genet. *9*, 1919–1926.

Cuff, J.A., Clamp, M.E., Siddiqui, A.S., Finlay, M., and Barton, G.J. (1998). JPred: a consensus secondary structure prediction server. Bioinformatics *14*, 892–893.

de la Fortelle, E., and Bricogne, G. (1997). Maximum-likelihood heavy-atom parameter refinement for multiple isomorphous replacement and multiwavelength anomalous diffraction methods. Macromol. Crystallogr. A *276*, 472–494.

Dodatko, T., Fedorov, A.A., Grynberg, M., Patskovsky, Y., Rozwarski, D.A., Jaroszewski, L., Aronoff-Spencer, E., Kondraskina, E., Irving, T., Godzik, A., and Almo, S.C. (2004). Crystal structure of the actin binding domain of the cyclase-associated protein. Biochemistry *43*, 10628–10641.

Fan, Y., Esmail, M.A., Ansley, S.J., Blacque, O.E., Boroevich, K., Ross, A.J., Moore, S.J., Badano, J.L., May-Simera, H., Compton, D.S., et al. (2004). Mutations in a member of the Ras superfamily of small GTP-binding proteins causes Bardet-Biedl syndrome. Nat. Genet. *36*, 989–993.

Farrar, G.J., Kenna, P.F., and Humphries, P. (2002). On the genetics of retinitis pigmentosa and on mutation-independent approaches to therapeutic intervention. EMBO J. *21*, 857–864.

Grayson, C., Bartolini, F., Chapple, J.P., Willison, K.R., Bhamidipati, A., Lewis, S.A., Luthert, P.J., Hardcastle, A.J., Cowan, N.J., and Cheetham, M.E. (2002). Localization in the human retina of the X-linked retinitis pigmentosa protein RP2, its homologue cofactor C and the RP2 interacting protein Arl3. Hum. Mol. Genet. *11*, 3065–3074.

Grynberg, M., Jaroszewski, L., and Godzik, A. (2003). Domain analysis of the tubulin cofactor system: a model for tubulin folding and dimerization. BMC Bioinformatics *4*, 46.

Haim, M. (2002). The epidemiology of retinitis pigmentosa in Denmark. Acta Ophthalmol. Scand. *80*, 5–34.

Hanzal-Bayer, M., Renault, L., Roversi, P., Wittinghofer, A., and Hillig, R.C. (2002). The complex of Arl2-GTP and PDE delta: from structure to function. EMBO J. *21*, 2095–2106.

Hardcastle, A.J., Thiselton, D.L., Van Maldergem, L., Saha, B.K., Jay, M., Plant, C., Taylor, R., Bird, A.C., and Bhattacharya, S. (1999). Mutations in the RP2 gene cause disease in 10% of families with familial X-linked retinitis pigmentosa assessed in this study. Am. J. Hum. Genet. *64*, 1210–1215.

Herrmann, C., Horn, G., Spaargaren, M., and Wittinghofer, A. (1996). Differential interaction of the ras family GTP-binding proteins H-Ras, Rap1A, and R-Ras with the putative effector molecules Raf kinase and Ral-guanine nucleotide exchange factor. J. Biol. Chem. *271*, 6794–6800.

Higgins, D.G., Thompson, J.D., and Gibson, T.J. (1996). Using CLUSTAL for multiple sequence alignments. Methods Enzymol. *266*, 383–402.

Holm, L., and Park, J. (2000). DaliLite workbench for protein structure comparison. Bioinformatics *16*, 566–567.

Holm, L., and Sander, C. (1993). Protein structure comparison by alignment of distance matrices. J. Mol. Biol. *233*, 123–138.

Hoyt, M.A., Stearns, T., and Botstein, D. (1990). Chromosome instability mutants of *Saccharomyces cerevisiae* that are defective in microtubule-mediated processes. Mol. Cell. Biol. *10*, 223–234.

Jones, T.A., Zou, J.Y., Cowan, S.W., and Kjeldgaard. (1991). Improved methods for building protein models in electron density maps and the location of errors in these models. Acta Crystallogr. A *47 (Pt 2)*, 110–119.

Kabsch, W. (1993). Automatic processing of rotation diffraction data from crystals of initially unknown symmetry and cell constants. J. Appl. Crystallogr. *26*, 795–800.

Kraemer, A., Rehmann, H.R., Cool, R.H., Theiss, C., de Rooij, J., Bos, J.L., and Wittinghofer, A. (2001). Dynamic interaction of cAMP with the Rap guanine-nucleotide exchange factor Epac1. J. Mol. Biol. *306*, 1167–1177.

Lin, W.D., Shi, Y.R., Tsai, F.J., Lee, C.C., Lin, H.J., and Wu, J.Y. (2001). Identification of a polymorphism (D168N) in the *XRP2* gene in Chinese. Hum. Mutat. *17*, 354.

Linari, M., Hanzal-Bayer, M., and Becker, J. (1999a). The delta subunit of rod specific cyclic GMP phosphodiesterase, PDE delta, interacts with the Arf-like protein Arl3 in a GTP specific manner. FEBS Lett. *458*, 55–59.

Linari, M., Ueffing, M., Manson, F., Wright, A., Meitinger, T., and Becker, J. (1999b). The retinitis pigmentosa GTPase regulator, RPGR, interacts with the delta subunit of rod cyclic GMP phosphodiesterase. Proc. Natl. Acad. Sci. USA *96*, 1315–1320.

Livingstone, C.D., and Barton, G.J. (1993). Protein sequence alignments: a strategy for the hierarchical analysis of residue conservation. Comput. Appl. Biosci. *9*, 745–756.

Mayer, U., Herzog, U., Berger, F., Inze, D., and Jurgens, G. (1999). Mutations in the pilz group genes disrupt the microtubule cytoskeleton and uncouple cell cycle progression from cell division in *Arabidopsis* embryo and endosperm. Eur. J. Cell Biol. *78*, 100–108.

Mears, A.J., Gieser, L., Yan, D., Chen, C., Fahrner, S., Hiriyanna, S., Fujita, R., Jacobson, S.G., Sieving, P.A., and Swaroop, A. (1999). Protein-truncation mutations in the RP2 gene in a North American cohort of families with X-linked retinitis pigmentosa. Am. J. Hum. Genet. *64*, 897–900.

Meindl, A., Dry, K., Herrmann, K., Manson, F., Ciccodicola, A., Edgar, A., Carvalho, M.R., Achatz, H., Hellebrand, H., Lennon, A., et al. (1996). A gene (RPGR) with homology to the RCC1 guanine nucleotide exchange factor is mutated in X-linked retinitis pigmentosa (RP3). Nat. Genet. *13*, 35–42.

Miano, M.G., Testa, F., Filippini, F., Trujillo, M., Conte, I., Lanzara, C., Millan, J.M., De Bernardo, C., Grammatico, B., Mangino, M., et al. (2001). Identification of novel RP2 mutations in a subset of X-linked retinitis pigmentosa families and prediction of new domains. Hum. Mutat. *18*, 109–119.

Murshudov, G.N., Vagin, A.A., Lebedev, A., Wilson, K.S., and Dodson, E.J. (1999). Efficient anisotropic refinement of macromolecular structures using FFT. Acta Crystallogr. D Biol. Crystallogr. *55*, 247–255.

Perrakis, A., Morris, R., and Lamzin, V.S. (1999). Automated protein model building combined with iterative structure refinement. Nat. Struct. Biol. *6*, 458–463.

Renault, L., Hanzal-Bayer, M., and Hillig, R.C. (2001). Coexpression, copurification, crystallization and preliminary X-ray analysis of a complex of ARL2-GTP and PDE delta. Acta Crystallogr. D Biol. Crystallogr. *57*, 1167–1170.

Roepman, R., van Duijnhoven, G., Rosenberg, T., Pinckers, A.J., Bleeker-Wagemakers, L.M., Bergen, A.A., Post, J., Beck, A., Reinhardt, R., Ropers, H.H., et al. (1996). Positional cloning of the gene for X-linked retinitis pigmentosa 3: homology with the guanine-nucleotide-exchange factor RCC1. Hum. Mol. Genet. *5*, 1035–1041.

Rose, R., Weyand, M., Lammers, M., Ishizaki, T., Ahmadian, M.R., and Wittinghofer, A. (2005). Structural and mechanistic insights into the interaction between Rho and mammalian Dia. Nature *435*, 513–518.

Rudolph, M.G., Linnemann, T., Grunewald, P., Wittinghofer, A., Vetter, I.R., and Herrmann, C. (2001). Thermodynamics of Ras/effector and Cdc42/effector interactions probed by isothermal titration calorimetry. J. Biol. Chem. *276*, 23914–23921.

Scheffzek, K., Ahmadian, M.R., Kabsch, W., Wiesmuller, L., Lautwein, A., Schmitz, F., and Wittinghofer, A. (1997). The Ras-RasGAP complex: structural basis for GTPase activation and its loss in oncogenic Ras mutants. Science *277*, 333–338.

Schwahn, U., Lenzner, S., Dong, J., Feil, S., Hinzmann, B., van Duijnhoven, G., Kirschner, R., Hemberger, M., Bergen, A.A., Rosenberg, T., et al. (1998). Positional cloning of the gene for X-linked retinitis pigmentosa 2. Nat. Genet. *19*, 327–332.

Sharon, D., Bruns, G.A., McGee, T.L., Sandberg, M.A., Berson, E.L., and Dryja, T.P. (2000). X-linked retinitis pigmentosa: mutation spectrum of the RPGR and RP2 genes and correlation with visual function. Invest. Ophthalmol. Vis. Sci. *41*, 2712–2721.

Shern, J.F., Sharer, J.D., Pallas, D.C., Bartolini, F., Cowan, N.J., Reed, M.S., Pohl, J., and Kahn, R.A. (2003). Cytosolic Arl2 is complexed with cofactor D and protein phosphatase 2A. J. Biol. Chem. *278*, 40829–40836.

Thiselton, D.L., Zito, I., Plant, C., Jay, M., Hodgson, S.V., Bird, A.C., Bhattacharya, S.S., and Hardcastle, A.J. (2000). Novel frameshift mutations in the RP2 gene and polymorphic variants. Hum. Mutat. *15*, 580.

Tian, G., Vainberg, I.E., Tap, W.D., Lewis, S.A., and Cowan, N.J. (1995). Quasi-native chaperonin-bound intermediates in facilitated protein folding. J. Biol. Chem. *270*, 23910–23913.

Tian, G., Huang, Y., Rommelaere, H., Vandekerckhove, J., Ampe, C., and Cowan, N.J. (1996). Pathway leading to correctly folded β-tubulin. Cell *86*, 287–296.

Tian, G., Lewis, S.A., Feierbach, B., Stearns, T., Rommelaere, H., Ampe, C., and Cowan, N.J. (1997). Tubulin subunits exist in an activated conformational state generated and maintained by protein cofactors. J. Cell Biol. *138*, 821–832.

Tian, G., Bhamidipati, A., Cowan, N.J., and Lewis, S.A. (1999). Tubulin folding cofactors as GTPase-activating proteins. GTP hydrolysis and the assembly of the α/β-tubulin heterodimer. J. Biol. Chem. *274*, 24054–24058.

Van Duyne, G.D., Standaert, R.F., Karplus, P.A., Schreiber, S.L., and Clardy, J. (1993). Atomic structures of the human immunophilin FKBP-12 complexes with FK506 and rapamycin. J. Mol. Biol. *229*, 105–124.

Vorster, A.A., Rebello, M.T., Coutts, N., Ehrenreich, L., Gama, A.D., Roberts, L.J., Goliath, R., Ramesar, R., and Greenberg, L.J. (2004). Arg120stop nonsense mutation in the RP2 gene: mutational hotspot and germ line mosaicism? Clin. Genet. *65*, 7–10.

Wada, Y., Nakazawa, M., Abe, T., and Tamai, M. (2000). A new Leu253Arg mutation in the RP2 gene in a Japanese family with X-linked retinitis pigmentosa. Invest. Ophthalmol. Vis. Sci. *41*, 290–293.

Yoder, M.D., Keen, N.T., and Jurnak, F. (1993). New domain motif: the structure of pectate lyase C, a secreted plant virulence factor. Science *260*, 1503–1507.

Zhao, Y., Hong, D.H., Pawlyk, B., Yue, G., Adamian, M., Grynberg, M., Godzik, A., and Li, T. (2003). The retinitis pigmentosa GTPase regulator (RPGR)-interacting protein: subserving RPGR function and participating in disk morphogenesis. Proc. Natl. Acad. Sci. USA *100*, 3965–3970.

Accession Numbers

The atomic coordinates and structure factors have been deposited in the Protein Data Bank with accession code 2BX6.